Contents lists available at ScienceDirect

Construction and Building Materials

journal homepage: www.elsevier.com/locate/conbuildmat

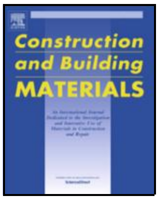

Construction and Building Materials 70 (2014) 339–350

Behavior of composite cement pastes containing silica nano-particles at elevated temperature

Mohamed Heikal [a,b,⇑], A.I. Ali [a], M.N. Ismail [c], S. Awad N.S. Ibrahim [d]

[a] Chemistry Department, Faculty of Science, Benha University, Benha, Egypt [b] Chemistry Department, College of Science, Al Imam Mohammad Ibn Saud Islamic University (IMSIU), P.O Box 90950, Riyadh 11623, Saudi Arabia [c] Polymer & Pigment Department, National Research Center, Dokki, Cairo, Egypt [d] Faculty of Engineering, Benha University, Benha, Egypt

highlights

- The compressive strength of OPC–GBFS–NS pastes increase with NS up to 4 %.
- Gel/space ratio of composite pastes increase with GBFS content up to 40 mass%.
- Free lime content of composite cement pastes increases up to 7 days then decreases.
- The compressive strength of mix IV.2 shows higher values up to 1000 C.
- Total porosity of composite pastes with 40% GBFS have lower values up to 1000 C.

article info

Article history:
Received 12 May 2014
Received in revised form 21 July 2014
Accepted 23 July 2014

Keywords:
Nano-silica
GBFS
Heat-treatment
Phase composition
Gel/space ratio

abstract

The work aims to study the effect of substitution of nano-silica (NS) on the behavior of composite cement pastes containing ordinary Portland cement (OPC) and blast-furnace slag (GBFS) exposed to elevated temperature up to 1000 C. The composite cements are composed of different amount of NS up to 6 mass% as well as 30–60 mass% GBFS. The behavior of hydration kinetics were studied for 1, 3, 7, 28 and 90 days. The fire resistance of composite cement pastes was evaluated for specimens cured for 28 days after firing at 250, 450, 600, 800 and 1000 C with rate of heating 3 C/min for 3 h soaking time, then cooled to room temperature in the furnace switched off. The compressive strength of OPC–NS and/or GBFS cement pastes increase with NS content up to 4%. Increases of the contents of NS up to 6% the values of compressive strength of OPC–NS cement pastes decreases. Gel/space ratio of OPC–GBFS–NS containing 4 mass% NS shows an increase with the increase of GBFS up to 40 mass% (mix IV.2). The compressive strength of III.2 and IV.2 show higher values at all thermally treatment temperature up to 1000 C. The compressive strength of the superplasticized OPC–NS–GBFS composite shows a higher values up to 1000 C in comparison with those pastes. It can be included that 30–60% GBFS in the presence of 4 mass% NS has a higher resistance to fire than all composite cement pastes.

1. Introduction

The applications of nano-technology have been gaining popularity in different fields of science and technology, especially in concrete industries. The developments of new materials within new functions or improvements in the properties of existing materials using nano-technology are new areas of interest in civil engineering [1,2]. These concrete products can already be seen today through many current applications such as surface coatings, self-cleaning capacity, and fire resistance [3]. The physical and chemical reactions, microstructure of concrete, improvement of these concretes and implementing novel methods employing materials with nano-scale are those within the dimension less than 100 nm. These nanomaterials can efficiently fill nano-pores in open pores system of hydrated cement mortars and increase strength of mortar aggregates, mortar-fibers interfaces resulting in an improved the structural properties of contact area and durability of concrete [4–9].

Nano-silica particles possessing high efficiency in concrete technology can improve structural properties of cement-based materials [10]. The behavior of these materials is mainly influenced by chemical reactions at the interface. Therefore, the use of nano-particles in concretes modify their behavior in the fresh and hardened conditions [11]. Nano-SiO_2 behaves not only as a filler to improve the microstructure of cement, but also as a promoter of pozzolanic reaction as well as an agent for improving the microstructure of the cement paste [12]. Nano-silica has proven to be an effective mineral addition for blending with Portland cement in order to improve the mechanical performance and the microstructure of high-strength cement pastes even in low concentration and this improvement of paste behavior is attributed to the fact that increasing packing among particles, and durability [5,13–16]. The incorporation of NS enhanced the compressive strength and tensile strength of mortar due to the increased pozzolanic action and filling effect. Moreover, incorporation of NS improved the microstructure of cement mortar [17]. Nano-silica accelerates the hydration reactions of

---

⇑ Corresponding author at: Chemistry Department, Faculty of Science, Benha University, Benha, Egypt.

E-mail address: ayaheikal@hotmail.com (M. Heikal).

http://dx.doi.org/10.1016/j.conbuildmat.2014.07.078 0950-0618/ 2014

cement phases as these particles are effective in filling the voids of the C– S–H, enhancing the rate of hydrations by acting as nucleation centers and reducing the size of $Ca(OH)_2$ crystal [1,18]. The use of NS was preferred in place of previously used pozzolanic material SF because the pozzolanic activity of the NS was more than SF at early days due to the higher of rate of consumption of $Ca(OH)_2$ crystals [5]. However, the addition of NS reduced the mix workability, due to immediate reaction between the NS and the cement paste, with development of gels characterized by high water retention capacities [19].

Colloidal-silica accelerated the cement hydration largely in the early age with a reduction in low-stiffness C–S–H gel and an increase in high-stiffness C–S–H gel [20] The application of colloidal-silica in concrete enhance the compressive strength, reduce of the porosity, due to fact that the addition of colloidal-silica led to the consumption of portlandite (CH) in the pozzolanic reaction, hence improving the concrete microstructure to become stronger and denser [21], as well as the permeability was also improved with addition of NS due to the removal of minute pores present in cement mortar matrix and ITZ [22]. Hosseini et al. [23] concluded that the replacing cement by 3% of NS of in the concrete made with 100% recycled aggregate produces strength more that of concrete made with natural aggregates. Moreover, microstructure became dense, uniform and even extremely small voids had been omitted due to the filling of small particles of NS in those voids.

Several studied have reported the effect of nano-materials in cement-based materials and, in general, they concluded that NS accelerate the chemical reactions during initial hydration [5,24– 32]. NS reacts with calcium hydroxide (CH) and increases the amount of calcium silicate hydrate (C–S–H) produced, leading to a compact microstructure and, consequently, improving the mechanical properties of hardened.

Fire is one of the natural hazards that attacks the building constructions. Subjecting concrete to a higher temperature (e. g., due to accidental fire etc.) leads to severe deterioration and it undergoes a number of transformations and reactions, thereby causing progressive breakdown of cement gel structure, reduced durability, increased tendency of drying shrinkage, and structural cracking [33]. The resistance of concrete exposure to elevated temperatures depends on the type of material used in the concrete. Both chemical and physical deteriorations occur at elevated temperatures because both interlayer and chemically bound water are lost due to the decomposition of calcium hydroxide (CH) and calcium silicate hydrate (C–S–H). Capillary and gel water evaporate at 100–150 C, shrinkage and cracking take place at approximately 150–250 C, accompanied by a reduction in tensile strength, evaporation of chemically bound water from aluminous and ferrous constituents at 250–300 C, and the compressive strength of concrete starts to decrease. CH dehydrates to calcium oxide at 400 C with an accompanying 44% reduction of the volume and a reduction in strength, C–S–H finishes decomposition between approximately 400 and 600 C, and strength reduction becomes significant. The effect of thermally treated temperatures up to 800 C on the physical properties, microstructure and phase composition of pozzolanic cement pastes [34–38]. The results show that additional hydration of unhydrated cement grains, recrystallization, deformation and transformation of CSH phases were occurred. The changes in physical state of cement pastes were studied by measuring deterioration in the compressive strength with temperature. The microstructure shows a massive dense closed texture, with the lower number of voids and pore size, with the formation of inner fibers and crystalline needle like CSH hydrated which is responsible for the increase in compressive strength up to 500 C [35]. Compressive strength decreased with the increase in temperature from 27 C to 800 C [39]. For all mixes, major strength and durability loss occurred after 400 C. Therefore, 400 C can be considered as critical temperature from the standpoint of strength and durability loss for change in the properties of cement mortar. The relative residual compressive strength was 88% at 450 C and 73% at 600 C, which was almost double than the residual strength shown by pure OPC pastes. This research showed that OPC–FA pastes performed better under elevated temperatures than OPC pastes [40]. The fire resistance of composite cement pastes was evaluated after firing at 250, 450 , 600, 800 C with rate of heating 3 C/min for 3 h soaking time. The physico-mechanical characteristics were determined at each firing temperature. The phase composition, free lime and microstructure for some selected samples were investigated. Cement pastes containing 10 and 15 mass% have higher firing resistance than all SF-pozzolanic cement pastes at 600 C [38]. It can be concluded that the composite cement pastes made from 10% of SF and 10%FA have good fire resistance in comparison with cement pastes made from only SF-pozzolanic cement pastes up to 450 C.

The increase of thermally treatment temperature from 25 C to 600 C, the compressive strength increases by 20.45–35.15% with superplasticizered OPC–SF cement pastes as well as with delaying addition times for 7.5–10 min, whereas the compressive strength decreases up to 800 C. The thermally treatment temperature increases from 600 C up to 800 C, a decreases compressive strength by 5.37–29.44% respectively for pastes admixed with delaying addition times in presence of 1.0–1.5 mass% of superplasticizer [41–43]. The increase of compressive strength up to 600 C, may be due to the acceleration of the hydration of pozzolanic reaction. The decrease at 800 C is due to the decomposition of cementitious materials and the coarsening of pore size distribution, which drastically increases the total porosity and decreases the bulk density.

The fire resistance of high strength fly ash (FA) mortar could be improved with addition of NS. The effect of high temperatures on the mechanical properties and microstructure of mortars containing NS and high-volume fly ash as a cement replacement was studied [44]. High residual strength after exposure to 700 C to that of control cement mortars before exposure to thermally treated temperature can be produced by replacing cement with FA–NS. Cement based materials have a stable microstructure state after exposure to temperatures up to 400 C. After exposure to thermally treated temperature, the pore size distribution significantly decreased for the FA–NS contained specimens; this new finding was detected by measuring the amount of nano-scale pores in the material after thermally treated temperature exposure, which refers to the production of more compact products.

The aim of the present work is to study the behavior of fire resistance characteristics of nano-silica–composite cement pastes thermally treated up to 1000 C.

2. Materials and experimental techniques

The starting materials used were ordinary Portland cement (OPC), granulated blast-furnace slag (GBFS), nano-silica (NS) and polycarboxylate based superplasticizer. The cement used in this study was the ASTM Type (I) ordinary Portland cement (OPC) provided from Lafarge Cement Company, Egypt. GBFS was supplied from Iron and Steel Company, Helwan, Egypt. Their chemical analyses are given in Table 1. The Blaine surface area of OPC and slag age particle size of 15 nm, 99.9 purity% was supplied from nanotechnology laboratory, Beni-Suief University, Beni-Suief, Egypt. XRD, and TEM of NS are given in Fig. 1. Superplasticizer was obtained from Sika Company, El-Abor City, Egypt. It is an opaque light yellow liquid with density 1.08 g/ml and chloride content <0.1 mass%.

The cement blends were mixed in a rotary mixer. NS are not easy to disperse uniformly due to their high surface energy. Accordingly, mixing was performed as follows; NS particles were stirred with the mixing water at high speed (120 rpm) for 1 min. The cement and GBFS (if applicable) were added to the mixer and mixed at medium speed (80 rpm) for another 30 s. The superplasticizer was added and stirred at high speed for additional 30 s. The mixture was allowed to rest for 90 s and then mixed for 1 min at high speed.

The mix compositions of the prepared cement blends are given in Table 2. The required water of standard consistency and setting times were measured according to ASTM specification [45]. The pastes were moulded in one inch cubic moulds, then strong manually pressed into the moulds. The specimens were cured in 100% RH chamber at a constant temperature 25 ± 1 C for the first 24 h and then immersed in tap water until the time of testing (1, 3, 7, 28 and 90 days). The hydration of cement pastes was stopped by pulverizing 10 g of representative sample in a beaker containing 1:1 (v/v) methanol–acetone mixture, then mechanically stirred for 1 h. The mixture was filtered through sintered glass G_4, after washing two times with the stopping solution and diethyl ether, then dried at 70 C for 1 h, then collected in polyethylene bags; sealed and stored in desiccators for analysis [46].

The samples subjected to thermally treated temperature were demoulded after 24 h, cured for 28 days under tap water, dried for 24 h at 105 C, then subjected to thermal treatment for 3 h at 250, 450, 600, 800 and 1000 C with heating rate 5 C/min, then cooled to room temperature in the furnace atmosphere. Bulk density and compressive strength of thermally treated cement pastes were determined after immersing the pastes overnight under kerosene [ISO-50/8, 198 3].

The combined water content is considered as the percent of ignition loss of the dried sample (on the ignited weight basis). Approximately 2 g of the pre-dried samples were ignited up to 1000 C for 1 h soaking time. The results of combined water contents were corrected for the water of free portlandite present in each sample [47]. Free lime contents of the hydrated cement pastes can be thermally determined. 0.5 g sample of the hardened cement was placed in a porcelain crucible introduced into a cold muffle furnace (room temperature). The temperature was increased up to 390 then to 550 C at heating rate of 3 C/min. The loss of weight occurred between 390 and 550 C with soaking time of 15 min is equal to the weight of water of calcium hydroxide. Therefore, the free portlandite can be calculated [46].

Bulk density was measured before the specimens subjected to compressive strength determination. Each measurement was conducted on at least three similar cubes of the same mix composition and curing time [48]. Compressive strength was determined according to (ASTM Designation: C-150, 2007) [49]. A set of three

Table 1
Chemical analysis of OPC, GBFS and NS (mass, %).

	SiO_2	Al_2O_3	Fe_2O_3	CaO	MgO	SO_3	Na_2O	K_2O	LOI	Total
OPC	19.3	3.94	3.8	62.67	1.90	3.22	0.44	0.22	3.04	98.53
GBFS	37.81	13.14	0.23	38.70	7.11	1.19	1.03	0.19	0.00	99.40
NS	98.61	0.01	0.01	0.01	0.01	0.29	0.3	0.045	0.71	99.99

Table 2
Mix compositions of the prepared composite cements, mass, %.

Mix no.	OPC	NS	GBFS	SP	Consistency,%	Setting times, min	
I.0	100	0	–	0.0	26.5	190	345
I.1	99	1	–	0.0	28.0	183	295
I.2	98	2	–	0.0	29.7	165	285
I.3	96	4	–	0.0	33.0	123	263
I.4	94	6	–	0.0	38.7	100	250
II.0	100	0	–	1.0	20.0	065	220
II.1	99	1	–	1.0	22.0	070	260
II.2	98	2	–	1.0	23.6	080	265
II.3	96	4	–	1.0	28.0	085	280
II.4	94	6	–	1.0	32.9	100	290
III.1	66	4	30	0.0	28.2	090	240
III.2	56	4	40	0.0	28.0	095	250
III.3	36	4	60	0.0	27.4	110	255
IV.1	66	4	30	1.0	19.0	064	240
IV.2	56	4	40	1.0	18.9	066	245
IV.3	36	4	60	1.0	18.0	080	255

were 3050 and 4000 cm /g, respectively. Nano-silica with the aver-

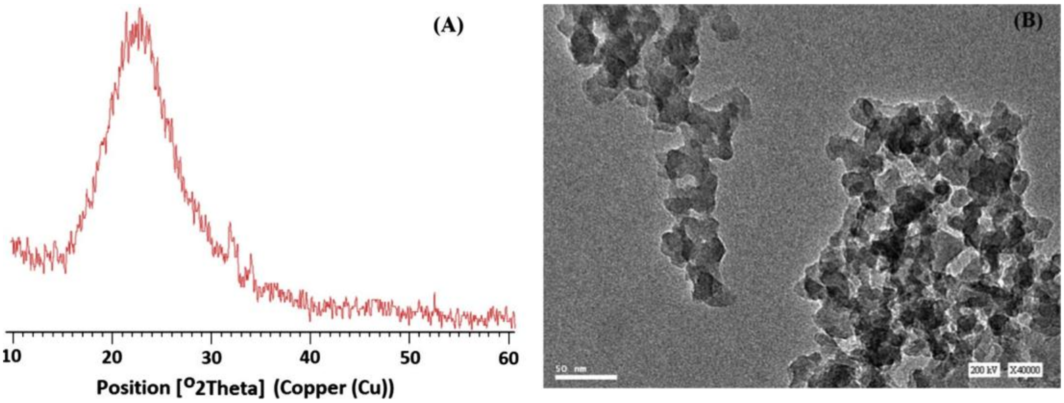

Fig. 1. XRD of and TEM of NS.

Initial set Final set

cubes was tested using compressive strength machine of SEIDNER, Riedinger, Germany, with maximum capacity of 2000 kN force.

The crystalline phases of cement pastes were identified using XRD technique of BRUXER, Axs D8 ADVANCE A8, and GERMANY Diffractometer. The samples were finely ground to pass a 200mesh sieve. The identification of all samples was confirmed by computer-aided search of the PDF database obtained from the Joint Committee on Powder Diffraction Standards-International Center for Diffraction Data (JCPDA-ICDD), 2001.

Thermal gravimetric analysis (TGA) was carried out using DTA50 Thermal Analyzer (Schimadzu Co., Tokyo, Japan). A dried sample of about 50 mg (53 lm) was used at heating rate 20 C/min under nitrogen atmosphere.

3. Results and discussion

3.1. Hydration behavior of composite cement pastes

3.1.1. Water of standard consistency and setting times

The variations of the required water of standard consistency and setting times of the fresh OPC and composite cement pastes containing 0, 1, 2, 4 and 6 mass% of NS or/and GBFS are represented in Table 2. It can be seen that the water demand increases with the increase of NS% content. The initial and final setting times of unsuperplasticized cement pastes were shorten with the addition of NS as shown in the behavior of mixes I. The setting is associated with the formation of calcium sulphoaluminate hydrates. The formation of AFt and AFm depends on the amount of aluminate phases, reaction velocity, rate of solution of $CaSO_4$ retarder, and CH liberated during the hydration of OPC phases (C_3S and b-C_2S). Addition of NS reduces the setting times.

The required water of standard consistency and setting times increase with increasing NS% as shown in mixes II. The initial and final setting times of superplasticized cement pastes were elongated. The retardation of setting processes is due to the presence of 1% superplasticizer [17]. The pastes containing NS require higher amounts of water of standard consistency more than the neat OPC paste [II.0] due to the high surface area of NS to form more hydrated products [8].

When NS is added to cement grains, $H_2SiO^2_4$ forms and reacts with the available Ca^{2+} which forms an additional amount of calcium silicate hydrate (C–S–H). C–S–H particles are spread in the water filled spaces between the cement grains and serve as seeds for the formation of more compact C–S–H phases.

Water of standard consistency as well as setting times of the prepared cement pastes, made of OPC–GBFS–NS mixes III and IV, are represented in Table 2. It can be seen that the water of standard consistency decreases, whereas initial and final setting times elongated with increasing the GBFS content, this is due to the lower hydraulic reactivity of GBFS in comparison with OPC during the very early ages of the hydration.

3.1.2. Chemically combined water contents

The variations of the chemically combined water contents of composite cement pastes hydrated up to 90 days as a function of NS contents was given in Fig. 2. Figure shows the variations of the chemically combined water contents of composite cement pastes with and without polycarboxylate superplasticizer. The degree of hydration is measured from the chemically combined water contents. Chemically combined water contents increase with the increase of curing age for all hydrated cement pastes; this is mainly due to the continuous of the hydration, leading to the formation of more excessive amounts of hydrated products, which precipitated in the available open pores system of the hardened cement pastes. The values of chemically combined water contents increase with increasing NS content up to 4 mass%. Increase of the contents of NS up to 6%, the chemically combined water content decreases, but still higher than that of the neat OPC paste. It is clear the chemically combined water contents of superplasticized pastes were decreased than those of unsuperplasticized pastes (Fig. 2B), this is attributed to the decrease of required water of standard consistency (mixing water).

NS particles have high surface area and contain many unsaturated bonds, which make them highly reactive, and water molecules are attracted towards the surface of these particles, as a result of this attraction, chemical bond is created between water and these particles along with formation of silanol groups (Si– OH). The increase in the required water of standard consistency is due to high surface energy of NS particles, which increase of the acceleration of the hydration process of cement phases [5,27]. The increase in chemically combined water contents in the presence of different contents of NS is mainly due to the higher pozzolanic activity of NS. NS reacts with the liberated CH during the hydration of cement phases to form additional hydrated products such as C–S–H, C–A–H and C–A–S–H. NS act as nucleation sites to accelerate the hydration, due to high surface area. NS accelerated the cement hydration largely in the early age with a reduction in low-stiffness C–S–H gel and an increase in highstiffness C–S–H gel [20]. The enhancement of NS is due to the filling of the voids of C–S–H structure, which leads to a denser and stronger concrete [22,23]. Acceleration of the hydration processes of cement pastes, and highly formation of CH during the initial period were shown [50].

OPC–GBFS cement pastes give relatively lower chemically combined water contents than those of OPC, especially at early hydration ages. But, at later ages (28–90 days) of the hydration of cement III.2 mix shows a higher values of chemically combined water contents than those of OPC–GBFS cement pastes; this is attributed to the higher activation of slag portion at longer curing times as shown in Fig. 2A,B. The data of the chemically combined water contents reflect the increase in hydration reaction rate for OPC– GBFS–NS composite cement pastes containing NS. The values of the chemically combined water contents increase with increasing NS content. Also, NS particles accelerate the hydration of cement, due to their high activity and nucleating effect [20]. The composite cement containing 4 mass% of NS (IV.2) has the highest values of chemically combined water contents, at all curing ages.

3.1.3. Free lime contents

The free lime contents of composite cement pastes containing different percentages of OPC–GBFS–NS up to 90 days are graphically represented in Fig. 3. The results indicate that the values of free lime of the neat OPC paste increase up to 90 days; the increase of the free lime values up to 90 days is due to the continuous hydration of the main cement phases (C_3S and b-C_2S), liberating CH as shown in Fig. 3A,B. Free lime content of composite containing OPC–NS and/or GBFS increases up to 3–7 days, then decreases up to 90 days. Fig. 3A shows the variation of free lime content of unsuperplasticized OPC–NS and/or GBFS pastes, these values increase up to 3 days, and then decrease with curing time up to 90 days, except the free lime of mix III.3 decreases up to 90 days. There are two processes; first is lime production from the hydration of cement clinker phases (C_3S and b-C_2S); second is the lime consuming (pozzolanic reaction). NS accelerates the hydration rate of cement phases (C_3S and b-C_2S), hence rate of CH liberation is higher than the rate of consumption by pozzolanic reaction with NS to produce additional C–S–H up to 3–7 days [27,51]. After 3 – 7 days up to 90 days the free lime decreases sharply due to the higher pozzolanic activity of NS or the rate of consumption is higher than that of liberation. NS, due to its high special surface, is so reactive, and produces C–S–H condensed gel as a result of

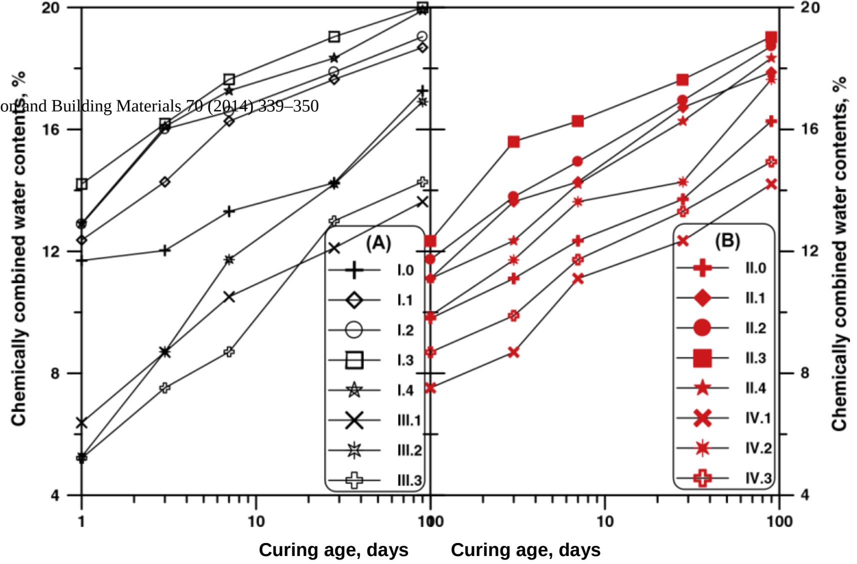

Fig. 2. Chemically combined water contents of hydrated composite cement pastes containing NS with curing time up to 90 days, (A) in the absence of superplasticizer; (B) in the presence of 1% superplasticizer.

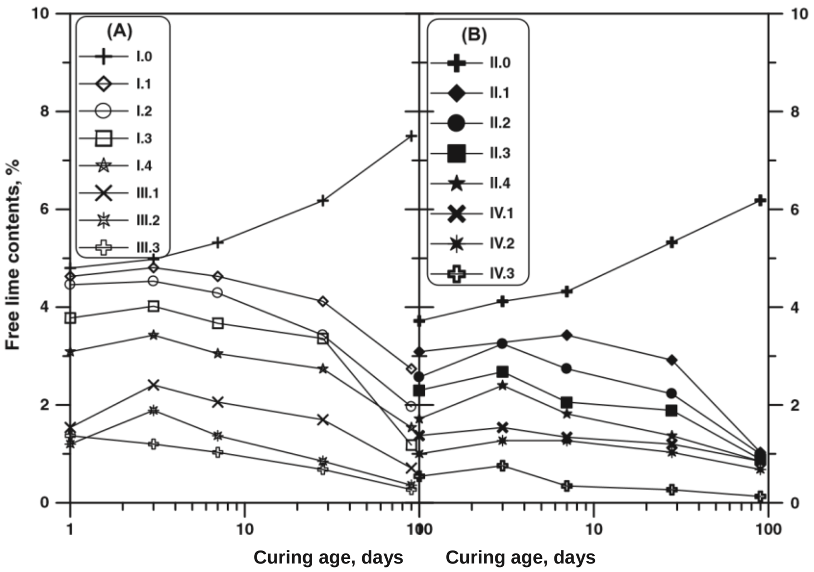

Fig. 3. Free lime contents of hydrated composite cement pastes containing NS with curing time up to 90 days, (A) in the absence of superplasticizer; (B) in the presence of polycarboxylate superplasticizer.

pozzolanic reaction. Therefore, in the pozzolanic reaction, the amount of crystals of CH decrease and high-strength dense gel C–S–H, which is a product of pozzolanic reaction [15,52–54]. GBFS also, reacted with the liberated free $Ca(OH)_2$ (lime consumption), the increase of the GBFS content decreases the values of lime consuming, hence the free lime content decreases.

The addition of NS in combination of superplasticizers results in the formation of low-density, dispersed-hydrated products of low C/S and low CH content, leading to relatively homogeneous composites. Superplasticizers improves the dispersion of both OPC and NS grains, leads to more efficient hydration and higher degree of compaction as well as it decrease the total porosity, which facilitate the approaching of NS from the lime released to form additional amounts of C–S–H, the free lime decreases as shown in Fig. 3B than those values of Fig. 3A.

3.1.4. Compressive strength

Compressive strength of composite cement pastes containing OPC–GBFS–NS up to 90 days are graphically represented in Fig. 4. The values of the compressive strength increase with curing time for all hydrated cement pastes, this is due to the continuous hydration and formation of excessive amounts of hydrated (C–S–H, C–A– H and C–A–S–H). These hydrates deposited in the available open pores forming a closed compact structure. The compressive strength of OPC–NS and/or GBFS cement pastes increase with NS content up to 4%. Increases of the contents of NS up to 6% the values of compressive strength of OPC–NS cement pastes decreases as shown in Fig. 4A,B.

Strength improvement is due to the increase in NS content, which can be attributed to the pozzolanic reaction, nano-filling, and acting as a nucleus [15,25,52,55], which improves the

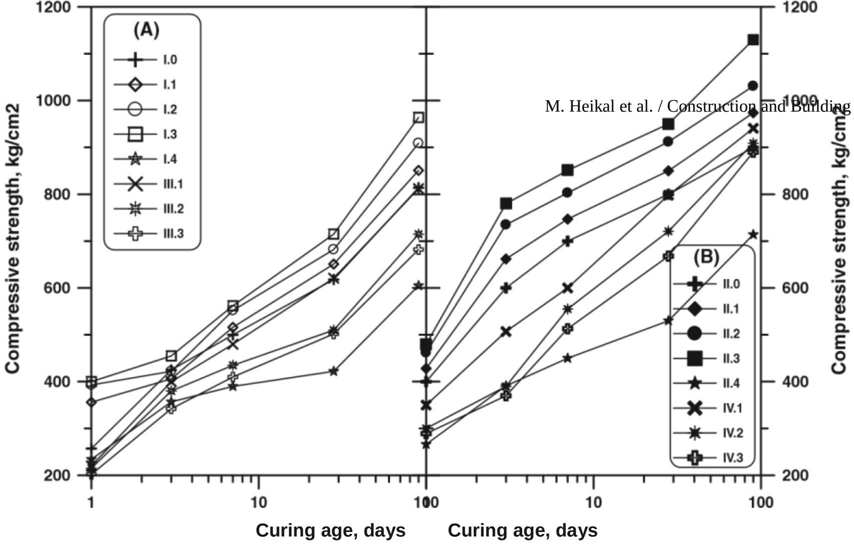

Fig. 4. Compressive strength of hardened composite cement pastes containing NS with curing time up to 90 days; (A) in the absence of superplasticizer; (B) in the presence of polycarboxylate superplasticizer.

microstructure and consequently increases in compressive strength values. As a result of this mechanism, NS due to its high special surface is so reactive and produces condensed C–S–H gel as a result of pozzolanic reaction with CH. Therefore, in the pozzolanic reaction, free CH decrease to produce additional dense C–S–H gel with high-strength. Increases the density of transition region/ area by filling empty spaces and thus increases the strength. Fast reactivity of NS grains is due to unsaturated bonds (Si–O–). Thus NS grains undergo quick reactions. NS fills the pores between C–S– H gel nanostructure (around 10 nm) to become closer and denser. NS acts also like nucleus forming an extremely strong bond with C–S–H gel particles, to form stable and durable hydrated products with higher compressive strength.

The compressive strength was developed in composite cement pastes containing NS particles higher than that of neat OPC cement pastes. The difference in the strength development is attributed to pozzolanic reaction. As mentioned above, nano-particles are thought to be more effective in pozzolanic reaction. Also, NS would fill pores to increase the compressive strength. Therefore, it is confirmed that the addition of NS to cement pastes improves their strength characteristics. Presence of superplasticizer the compressive strength of composite cement pastes increases as shown in Fig. 4B. In presence of superplasticizer, the required water of standard consistency as well as initial total porosity decrease, which facilitate the approaching of NS from the lime released as a result of the hydration of cement phases (C_3S and b-C_2S) to form additional amounts of C–S–H with low C/S and low $Ca(OH)_2$ content, leading to relatively homogeneous composites. The use of superplasticizers improves the dispersion of OPC, GBFS and NS grains, leads to more efficient hydration and higher degree of compaction.

3.1.5. Gel space ratio

The strength of the pastes is affected by W/C ratio, degree of hydration, air content and temperature. The strength can be correctly related to the solid hydration products and to the space available for formation of these products. The gel/space ratio (X) is represented by the following equation [56–57]:

$$X ¼ \frac{2:06V_c a}{V_c a þ W_o=C} \quad ð1Þ$$

where C = mass of the cement, V_c = specific volume of cement = 0.319 c.c./gm, W_o = mass of mixing water and a = the degree of the hydration. The degree of hydration is defined as:

$$a ¼ \frac{W^n}{{}_1 W_n} \quad ð2Þ$$

where W^1_n is the chemically combined water content after complete hydration, W_n is the chemically combined water content at any time of hydration.

The gel/space ratio (X) of the hardened neat and superplasticized cement pastes was calculated at various degrees of hydration and their W/C ratios as:

$$X ¼ \frac{0:647a}{0:319aþW_o=C} \quad ð3Þ$$

The gel/space ratios (X) of the hardened OPC–NS and/or GBFS composite cement pastes were calculated on the basis of the degrees of hydration and their W/C ratios; the gel/space ratios was given in Fig. 5. On increasing the gel/space ratio, the amount of hydration products increases; consequently, the compressive strength of the cement pastes enhances. As NS content increase, the gel/space ratio as well as the degree of hydration increases. The gel/space ratios (X) of the hardened OPC–NS composite cement pastes increases with NS content up to 4 mass% in the in absence and presence of polycarboxylate superplasticizer as shown in Fig. 5A,B. Fig. 5B shows an enhancement in gel/space ratio of superplasticized OPC–NS and/or GBFS composite cement pastes, this is due to the production of more dense and close-textured structure of cement pastes including NS leads to an increase in the rate of hydration of cement particles. Gel/space ratio of OPC– GBFS–NS containing 4 mass% NS shows an increase with the increase of GBFS up to 40 mass% (mix IV.2) as shown in Fig. 5A,B.

3.1.6. XRD diffraction patterns

X-ray diffractograms of the hardened I.3, II.3, IV.1, IV.2 and IV.3 composite cement pastes containing 4 mass% NS hydrated for 90 days are shown in Fig. 6. Fig. 6 shows the presence of diffraction lines corresponding to hydrated and anhydrated phases namely, CH, b-C_2S, C_3S, $C\overline{C}$ and CSH. As the hydration proceeds, the peak intensity of C–S–H increases, whereas those peaks of CH decrease; this is due to pozzolanic reaction of NS with the released portlandite during OPC cement hydration. Mix II.3 exhibits lower intensity of portlandite and higher intensity of diffraction lines of characteristics for CSH peaks in comparison with those of mix I.3.

XRD patterns corresponding to IV.1, IV.2, and IV.3 hydrated for 90 days as shown in Fig. 6. The diffraction patterns deposited the

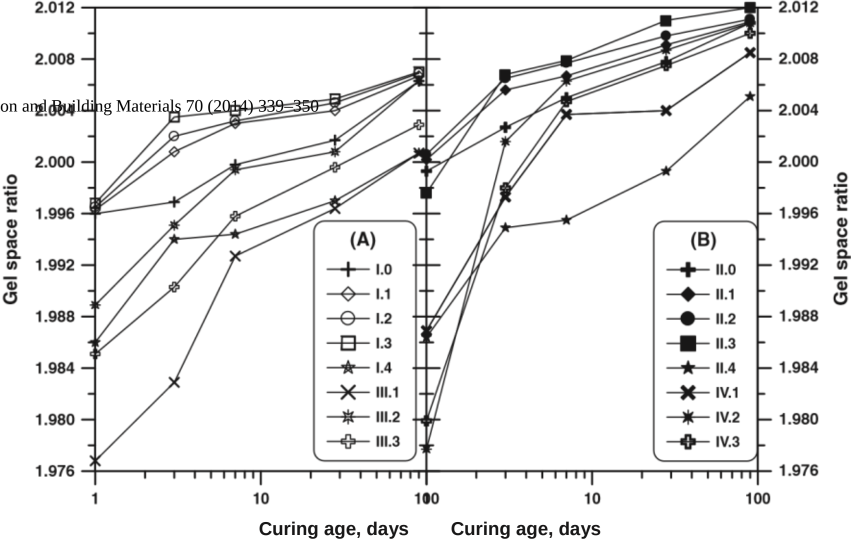

Fig. 5. Gel space ratio of hardened composite cement pastes containing NS with curing time up to 90 days; (A) in the absence of superplasticizer; (B) in the presence of polycarboxylate superplasticizer.

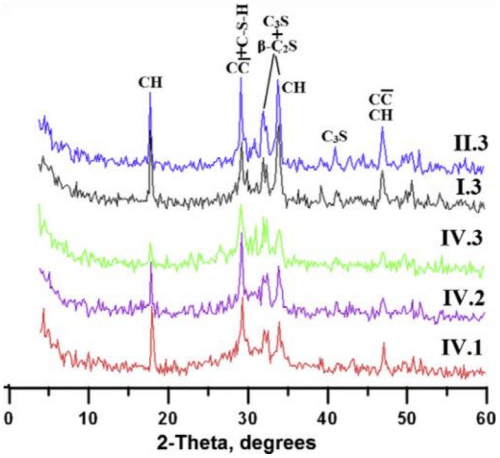

Fig. 6. XRD patterns of hardened composite cement pastes containing NS with curing time up to 90 days.

presence of anhydrous calcium silicate phases peaks superpose with the presence of hydrated phases such as C–S–H and CH peaks. OPC–GBFS–NS composite cement pastes (IV.3) exhibit lower intensity of portlandite peaks in comparison with those of IV.1 and IV.2. Therefore, the rate of lime consumption and that of CSH production increase in the presence of 4 mass% NS and 40% GBFS, this result confirms the increase of compressive strength and gel space ratio as shown in Figs. 4 and 5.

3.2. Behavior of composite cement pastes at elevated temperature

3.2.1. Ignition loss

Fig. 7 shows ignition loss of the hardened OPC–NS and/or GBFS composite cement pastes as a function of treatment temperature up to 1000 C. The evaporable water was removed at 105 C, a partial decomposition of C–S–H, C–A–H and sulphoaluminate hydrates occurred up to 200 C, moreover the decomposition of gehlenite hydrate (C_2ASH_8) above 200 C and dehydration of CH at nearly 400–550 C. The decarbonation of $C\overline{C}$ occurred between 650 and 800 C [38]. The results indicate that ignition loss is sharply increased up to 250 C due to the removal of free, adsorbed and bound water of cement pastes. As temperature increases, the ignition loss slightly increases up to 1000 C. This is due to the decomposition of some hydrated products, such as C–S–H and calcium sulphoaluminate, and gehlenite like hydrate (C_2ASH_8) as well as dehydration of CH at temperature 400–500 C [38,58]. Mixes containing GBFS shows an increase in the ignition loss from 250 to 450 C due to the higher pozzolanic activity to form additional C–S–H hydrated products as shown in Fig. 7. It was reported that the addition of 4 mass% NS acts as a nucleating agents which activates OPC–NS–GBFS composite cement to react with liberated CH, forming thus an additional C–S–H hydrated products.

3.2.2. Compressive strength

The variation of compressive strength of the hardened OPC–NS and/or GBFS composite cement pastes as a function of treatment temperature up to 1000 C is graphically represented in Fig. 8. The compressive strength increases with thermally treatment temperature up to 450 C then decrease for all OPC–NS–GBFS composite cement pastes, then decreases up to 1000 C for all cement pastes. The compressive strength of III.2 and IV.2 show higher values at all thermally treatment temperature up to 1000 C. This is due to higher consumption of portlandite. The compressive strength of OPC–NS–GBFS composite increases as a result of enhancing the hydration of unhydrated cement clinker [59]. This is attributed to the internal autoclaving effect that builds up as a result of flow of produced steam from elimination of capillary, physically adsorbed and bound water in cement pastes at high temperature that forms internal autoclaving reaction giving hydration products as well as improvement of pozzolanic reaction of NS with CH to form additional C–S–H with low Ca/Si ratio with high strength [60,61]. Whereas, the compressive strength decreases at 800–1000 C, may be ascribed to the decomposition of cementitous materials such as C–S–H as well as swelling of the water layer in the cement pastes. As the treatment temperature increases up to 1000 C, the porosity of cement pastes increases due to the coarsening of the pore size distribution. The decomposition of these hydrates takes place at thermally treatment temperature up to 1000 C to form crystalline structure similar to C_2S as well as formation of gehlenite and wallastonite crystalline phases. These crystalline phases opening the pore system leading to increase the porosity and decreases the compressive strength.

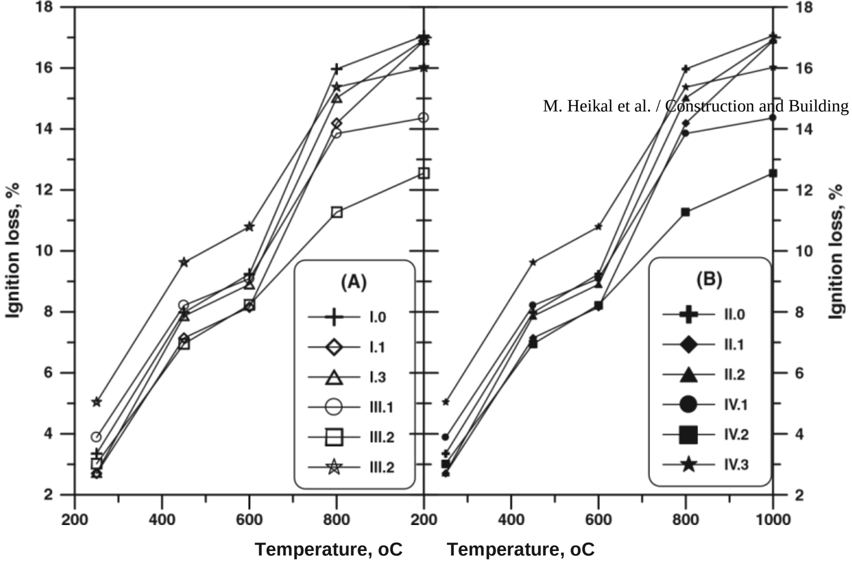

Fig. 7. Ignition loss of hardened composite cement pastes containing NS as a function of treatment temperature up to 1000 C; (A) in the absence of superplasticizer; (B) in the presence of polycarboxylate superplasticizer.

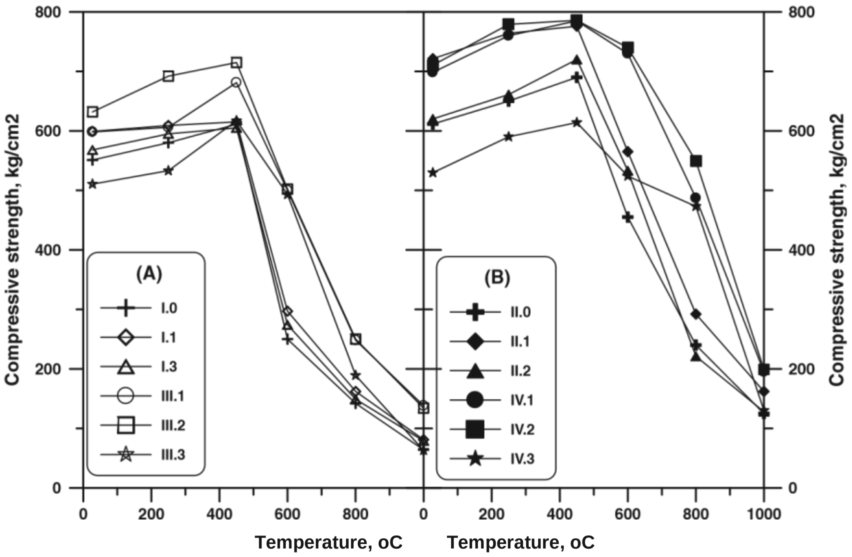

Fig. 8. Compressive strength of hardened composite cement pastes containing NS as a function of treatment temperature up to 1000 C, (A) in the absence of superplasticizer; (B) in the presence of polycarboxylate superplasticizer.

The compressive strength of the superplasticized OPC–NS–GBFS composite shows a higher values up to 1000 C in comparison with those pastes as shown in Fig. 8B. Generally, the partial substitution of OPC by 30–60% GBFS improves the compressive strength of cement pastes at 800 C. It can be included that 30–60% GBFS in the presence of 4 mass% NS has a higher resistance to fire than all composite cement pastes.

3.2.3. Bulk density

The bulk density of thermally treated temperature OPC–NS–GBFS composite containing different amounts of NS and GBFS were represented as a function of treatment temperature in Fig. 9. The change of bulk density of composite cement pastes with treatment temperature takes place in three steps. The first step, the bulk density decreases up to 450 C due to the removal of free, adsorbed and chemically combined water of C–S–H, C–A–H, and calcium aluminosilicate hydrates. Within the temperature range up to 600 C, mix I has higher values of bulk density. This is due to the higher values of hydration products from the cement clinker phases as shown in Fig. 9A. The second step takes place from 450 to 600 C, the bulk density has almost the same values. During this step (second step) the decomposition of CH. As the pozzolanic reaction takes place, these composite cement reacted with most CH liberated to form additional C–S–H, C–A–H and C_2ASH_8 phases. These products precipitated within the open pore system to form more compact close and dense structure. The third step (from 600 to 1000 C) is accompanied by an increase in the bulk density for all cement pastes due to the decomposition of CC to $\bar{C}aO$ and CO_2. Increase of the temperature above 600–1000 C caused strong losses and significant coarsening of the pore size distribution [62], this leads to the formation of denser structure, with associated shrinkage, evidently, total porosity increases as well as bulk density increases. The increase of bulk density due to the sintering from solid state decomposed CaO to give dense mater.

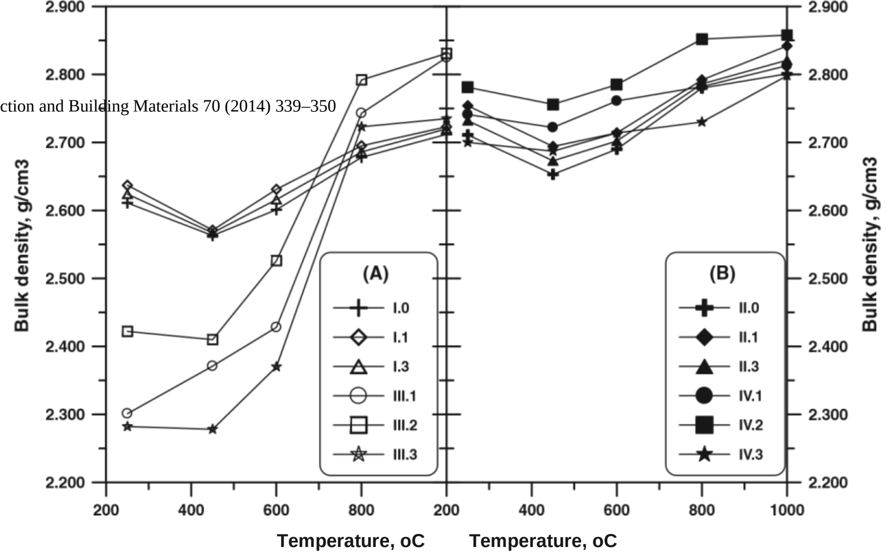

Fig. 9. Bulk density of hardened composite cement pastes containing NS as a function of treatment temperature up to 1000 C, (A) in the absence of superplasticizer; (B) in the presence of polycarboxylate superplasticizer.

Generally, bulk density of cement pastes increase up to 450– 800 C, due to the self-autoclaving reaction of NS with CH and/or the hydration of anhydrous cement grains forming more cementituous materials that fill some pores producing closed compact structure. The bulk density of superplasticized OPC–NS–GBFS composite containing different amounts of NS and GBFS were represented as a function of treatment temperature in Fig. 9B. Mixes IV.1 and IV.2 show the highest values of bulk density (Fig. 9B). The use of superplasticizers improves the dispersion of both OPC, GBFS and NS grains, leads to more efficient hydration and higher degree of compaction, which facilitate the approaching of NS from the lime released as a result of the hydration of cement phases (C_3S and bC_2S) to form additional amounts of C–S–H with low C/S and low

CH content, leading to relatively homogeneous composites. The increase of bulk density of these mixes, is due to the increase of the stability of the hydration products which formed up to 1000 C.

3.2.4. Total porosity

Total porosity of OPC–NS–GBFS composite cement pastes as a function of treatment temperature is presented in Fig. 10. Total porosity decreases with thermally treatment temperature up to 250 C, due to that the thermally treatment temperature enhances the hydration of unhydrated cement phases as well as the reaction of NS and GBFS with CH to form additional hydration products that fill the available open pores [34,35,37,38]. The total porosity increases sharply with treatment temperature from 250 C up to 1000 C for all cement pastes as a result of the formation of micro-cracks and/or increase of degree of crystallinity of the formed hydrates leading to a sort of opening of the pore system of cement pastes [37]. Total porosity decreases with NS content; this is attributed to the consumption of CH to form more hydration products. Also, the porosity increases sharply up to 600–800 C, due to a significant increase of microcracks. The porosity increases rapidly due to the decomposition of CH at 600 C. The increase of total porosity after 600 C up to 1000 C is due to the decomposition of some carbonated C–S–H in addition to the other hydration products. Exposed temperature above 600 C up to 1000 C caused strength losses and significant coarsening as a result of sintering. The increase in temperature affects on the pore size distribution. The decrease of compressive strength can be connected to the increase of porosity. The basic phenomena governing changes of cement based materials at high treatment temperature are known desiccation of pore system, opposite thermal deformation, chemical phase transformation, decomposition of hydrated products and destruction of microstructure. The data show that unsuperplasticized III.1 and III.2 as well as superplasticized IV.1 and IV.2 mixes have lower values of total porosity than those of other composite cement pastes up to 1000 C. Composite cement pastes containing NS acts as a nucleating site that increases the rate of hydration as well as reacting with the CH forming CSH products.

3.2.5. X-ray analysis

Figs. 11 and 12 show XRD diffraction patterns of specimens I.0 (OPC) and I.3 (96% OPC + 4 mass% NS). XRD diffraction patterns of I.0 at 250 C shows the main phases as C–S–H gel, unhydrated

C_3S and b-C_2S, CH and CC. The diffraction lines due to CH at 4.92 , 2.62, 1.92 and 1.79 Å showed that the intensities of diffraction lines corresponding to CH of mix I.3 (4 mass% NS) are less than the intensities of diffraction lines corresponding to I.0 (0% NS). Also, the intensity of diffraction lines corresponding to C–S–H of I.3 is higher than I.0 up to 600 C. The intensities diffraction lines corresponding to anhydrous phases (C_3S and b-C_2S) are lower for I.3 than I.0. It was concluded that I.3 has more hydration products than I.0. The decrease intensities diffraction lines corresponding of CH at 450 C is mainly due to the thermal hydration process that proceed as a result of self-autoclaving to produce additional hydration products as a result of reaction of CH with NS. This pozzolanic reaction occurred at 250–450 C leads to form additional C–S–H, C–A–H and gehlenite like hydrate (C_2ASH_8). The lines characteristic of C–S–H are overlapped with the lines of CC. At 600 C the intensity of diffraction lines due to CH is hardly defected for I.3 than I.0, where the line corresponding to C–S–H and CC increases, due to some of CH were transformed from CH to CC. It is difficult to differentiate the peaks of b-C_2S and C_3S from cement which has suffered decomposition, and the amounts of b-C_2S and C_3S formed during the decomposition from thermally treatment [35,37,63]. This indicates that C–S–H transforms at high temperature to the thermally stable forms similar to b-C_2S and C_3S minerals. On the other side, the intensity of CC peak removed at 1000 C as a result of partial decomposition to CaO. At 1000 C, C–S–H has completely disappeared, this is mainly due to the transformation to crystalline anhydrous calcium silicate phases [35,37,63]. This hypothesis is sustained by the parallel increase in the intensity peaks of b-C_2S and C_3S at 600–1000 C. The presence of portlandite at 1000 C is due to the rehydration of lime (CaO) for I.0 specimen.

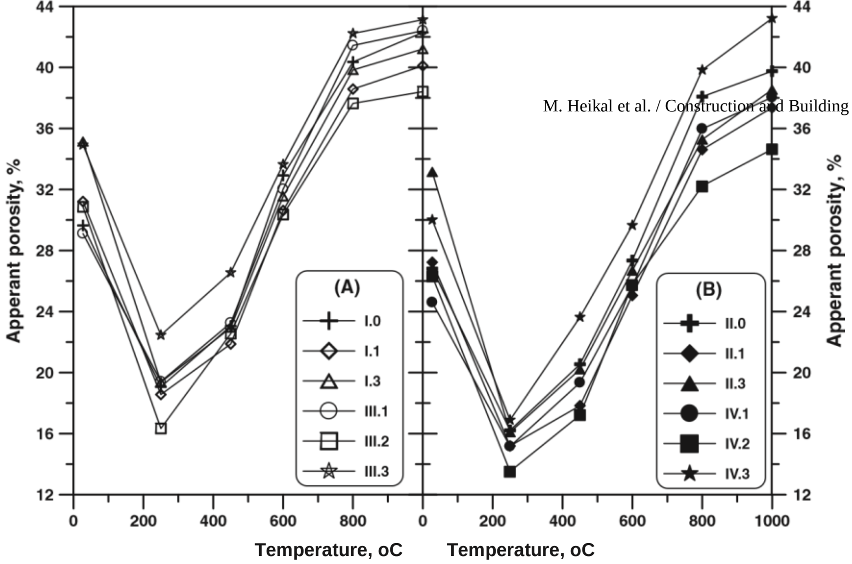

Fig. 10. Total porosity of hardened composite cement pastes containing NS as a function of treatment temperature up to 1000 C, (A) in the absence of superplasticizer; (B) in the presence of polycarboxylate superplasticizer.

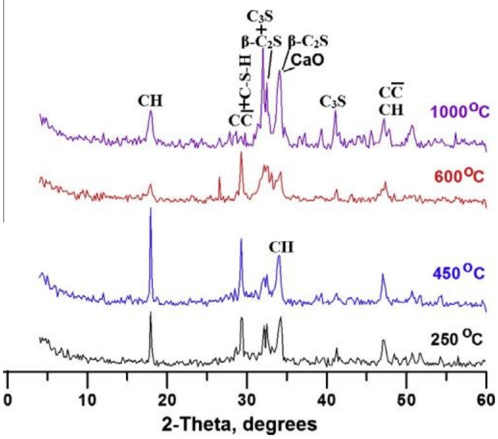

Fig. 11. XRD patterns of I.0 (OPC) as a function of treatment temperature up to 1000 C.

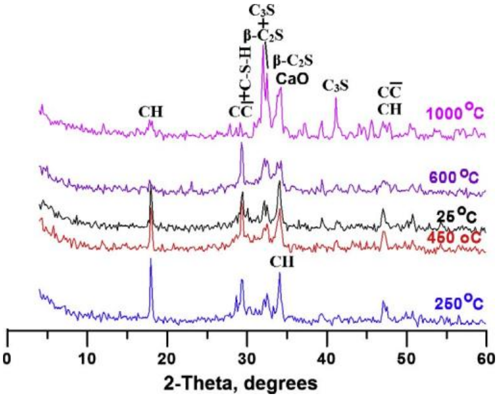

Fig. 12. XRD patterns of I.3 cement pastes containing 4 mass% of NS as a function of treatment temperature up to 1000 C.

XRD diffractograms of I.3 thermally treated at 600–1000 C are given in Fig. 12. XRD diffraction patterns of the paste containing I.3 indicates the formation of wollastonite ($CaOSiO_2$) in addition to bC_2S and C_3S. The disappearance of CH and the presence of higher amounts of CSH are evidenced that NS consumes CH forming additional C–S–H gel. It was concluded that the diffraction lines of crystalline wollastonite at 1000 C are detected, due to the high pozzolanic activity of NS to form more additional products from the pozzolanic reaction to form C–S–H, not from the decomposition of C–S–H from OPC hydration. It is well known that the decomposition of CSH phase which formed from the pozzolanic reaction forms crystalline monocalcium silicate (wollostonite) at 3.82511, 3.49396, 2.97552, 1.82988 and 1.71621 Å. Wollastonite is a ceramic product; therefore, these cements are durable and give reasonable higher compressive strength.

4. Conclusions

From the above findings it can concluded that:

A. Behavior of pozzolanic cement pastes containing microsilica:

1. The initial and final setting times of unsuperplasticized cement pastes were shorten with the addition of NS. Addition of NS reduces the setting times, whereas elongated for superplasticized cement pastes as well as for OPC–GBFS–NS mixes III and IV.
2. The values of chemically combined water contents increase with increasing NS content up to 4 mass%. The OPC–GBFS–NS composite cement containing 4 mass% of NS (IV.2) has the highest values of chemically combined water contents, at all curing ages.
3. Free lime content of composite containing OPC–NS and/or GBFS increases up to 3–7 days, then decreases up to 90 days.
4. The compressive strength of OPC–NS and/or GBFS cement pastes increase with NS content up to 4 %.
5. Gel/space ratio of OPC–GBFS–NS containing 4 mass% NS shows an increase with the increase of GBFS up to 40 mass% (mix IV.2).
6. OPC–GBFS–NS composite cement pastes (IV.3) exhibit lower intensity of portlandite peaks in comparison with those of IV.1 and IV.2.

B. Behavior of composite cement pastes at elevated temperature

1. Mixes containing GBFS shows an increase in the ignition loss from 250–450 C due to the higher pozzolanic activity to form additional C–S–H hydrated products. 4 mass% NS acts as a nucleating agents which activates OPC–NS–GBFS composite cement to react with liberated CH, forming thus an additional C–S–H hydrated products.
2. The compressive strength of III.2 and IV.2 show higher values at all thermally treatment temperature up to 1000 C. It can be concluded that 30–60% GBFS in the presence of 4 mass% NS has a higher resistance to fire than all composite cement pastes. 3. Mixes IV.1 and IV.2 show the highest values of bulk density.
4. The data show that unsuperplasticized III.1 and III.2 as well as superplasticized IV.1 and IV.2 mixes have lower values of total porosity than those of other composite cement pastes up to 1000 C.

References

[1] Sanchez F, Sobolev K. Nanotechnology in concrete – a review. Constr Build Mater 2010;24(11):2060–71.

[2] Pacheco-Torgal F, Jalali S. Nanotechnology: advantages and drawbacks in the field of construction and building materials. Constr Build Mater 2011;25(2):582–90.

[3] Leydecker S, Kölbel M, Peters S. Nano materials in architecture, interior architecture and design. Berlin: Birkhäuser; 2008.

[4] Wiesner MR, Bottero JY. Environmental nanotechnology: applications and impacts of nanomaterials. New York: McGraw-Hill; 2007.

[5] Qing Y, Zenan Z, Deyu K, Rongshen K. Influence of nano-SiO_2 addition on properties of hardened cement paste as compared with silica fume. Constr Build Mater 2007;21:539–45.

[6] Li G. Properties of high-volume fly ash concrete incorporating nano-SiO_2. Cement Concr Res 2004;34:1043–9.

[7] Aly M, Hashmi MSJ, Olabi AG, Messeiry M, Abadir EF, Hussain AI. Effect of colloidal nano-silica on the mechanical and physical behavior of waste-glass cement mortar. Mater Des 2012;33:127–35.

[8] Ali Nazari, Shadi Riahi. The effects of SiO_2 nanoparticles on physical and mechanical properties of high strength compacting concrete. Composites: Part B 2011;42:570–8.

[9] Behtash Amiri, Ali Bahari, Nik Aref Sadeghi, Nik Adel Sadeghi, Movahedi Naser Salman. Use of AFM technique to study the nano-silica effects in concrete mixture. Indian J Sci Technol 2012;5(2):2055–9.

[10] Beigi MH, Berenjian J, Omran OL, Nik AS, Nikbin IM. An experimental survey on combined effects of fibers and nanosilica on the mechanical, rheological, and durability properties of self-compacting concrete. Mater Des 2013;50:1019–29.

[11] Senff L, Labrincha JA, Ferreira VM, Hotza D, Repette WL. Effect of nano-silica on rheology and fresh properties of cement pastes and mortars. Constr Build Mater 2009;23:2487–91.

[12] Choolaei M, Rashidi AM, Yadegari MA, Soltanian H. The effect of nanosilica on the physical properties of oil well cement. Mater Sci Eng A 2012;538:288–94.

[13] Stefanidou M, Papayiann I. Influence of nano-SiO_2 on the Portland cement pastes. Compos Part B: Eng 2012;43(6):2706–10.

[14] Tobón JI, Restrepo OJ, Payá J. Comparative analysis of performance of Portland cement blended with nanosiliaca and silica fume. Dyna 2010;77(163):37–46.

[15] Ji T. Preliminary study on the water permeability and microstructure of concrete incorporating nano-SiO_2. Cem Concr Res 2005;35(10):1943–7.

[16] Gaitero JJ, Campillo I, Guerrero A. Reduction of the calcium leaching rate of cement paste by addition of silica nanoparticles. Cem Concr Res 2008;38(8– 9):1112–8.

[17] Jo BW, Kim CH, Tae Gh, Park JB. Characteristics of cement mortar with nanoSiO2 particles. Constr Build Mater 2007;21(6):1351–5.

[18] Pacheco-Torgal F, Miraldo S, Ding Y, Labrincha JA. Targeting HPC with the help of nanoparticles: an overview. Constr Build Mater 2013;38:365–70.

[19] Berra M, Carassiti F, Mangialardi T, Paolini AE, Sebastiani M. Effects of nanosilica addition on workability and compressive strength of Portland cement pastes. Constr Build Mater 2012;35:666–75.

[20] Hou P, Kawashima S, Kong D, Corr DJ, Qian J, Shah SP. Modification effects of colloidal nano-SiO_2 on cement hydration and its gel property. Compos Part B: Eng 2013;45(1):440–8.

[21] Said AM, Zeidan MS, Bassuoni MT, Tian Y. Properties of concrete incorporating nano-silica. Constr Build Mater 2012;36:838–44.

[22] Zhang MH, Li H. Pore structure and chloride permeability of concrete containing nano-particles for pavement. Constr Build Mater 2011;25(2):608–16.

[23] Hosseini P, Booshehrian A, Madari A. Developing concrete recycling strategies by utilization of nano-SiO_2 particles. Waste Biomass Valorization 2011;2(3):347–55.

[24] Lin KL, Chang WC, Lin DF, Luon HL, Tsai MC. Effects of nano-SiO_2 and different ash particle sizes on sludge ash–cement mortar. J Environ Manage 2008;88:708–14.

[25] Li H, Gang H, Jie X, Yuang J, Ou J. Microstructure of cement mortar with nanoparticles. Compos Part B: Eng 2004;35:185–9.

[26] Li G. Properties of high-volume fly ash concrete incorporating nano-SiO_2. Cem Concr Res 2004;34:1043–9.

[27] Björnström J, Martinelli A, Matic A, Börjesson L, Panas I. Accelerating effects of colloidal nano-silica for beneficial calcium–silicate–hydrate formation in cement. Chem Phys Lett 2004;392(1–3):242–8.

[28] Shih JY, Chang TP, Hsiao TC. Effect of nanosilica on characterization of Portland cement composite. Mater Sci Eng A 2006;424:266–74.

[29] Chen J, Poon Chi-sun. Photocatalytic construction and building materials: From fundamentals to applications. Build Environ 2009;44:1899–906.

[30] Ruot B, Plassais A, Olive F, Guillot L, Bonafous L. TiO_2-containing cement pastes and mortars: Measurements of the photocatalytic efficiency using a rhodamine B-based colourimetric test. Sol Energy 2009;83:1794–801.

[31] Hassan MM, Dylla H, Mohammad LN, Rupnow T. Evaluation of the durability of titanium dioxide photocatalyst coating for concrete pavement. Constr Build Mater 2010;24:1456–61.

[32] Hüsken G, Hunger M, Brouwers HJH. Experimental study of photocatalytic concrete products for air purification. Build Environ 2009;44:2463–74.

[33] Andiç-Çakır Özge, Çopurog˘lu Og˘uzhan, Ramyar Kambiz. Effect of high temperature on mechanical and microstructural properties of cement mortar. In: 11DBMC International conference on durability of building materials and components, Istanbul, Turkey 11–14, T11; May 2008.

[34] Heikal M. Effect of temperature on the physico-mechanical and mineralogical properties of Homra pozzolanic cement pastes. Cem Concr Res. 2000;30:1835–9.

[35] Heikal M. Effect of elevated temperature on the physico-mechanical and microstructural properties of blended cement pastes. Build Res J 2008;56(2):157–72.

[36] El-Didamony H, Heikal M, El-sokkary TM, Abdallah Moustafa M. Effect of fire on the deterioration of Portland and blended cements. HBRC J 2007;3(3):23–33.

[37] Heikal M. Effect of temperature on structure and strength properties of cement pastes containing fly ash in combination with limestone. Ceramics-Silikáty 2006;50(3):163–73.

[38] Heikal M, El- Didamony H, Sokkary TM, Ahmed IA. Behavior of composite cement pastes containing microsilica and fly ash at elevated temperature. Constr Build Mater 2013;38:1180–90.

[39] Nadeem A, Memon SA, Lo TY. Mechanical performance, durability, qualitative and quantitative analysis of microstructure of fly ash and Metakaolin mortar at elevated temperatures. Constr Build Mater 2013;38:338–47.

[40] Aydin S, Baradan B. Effect of pumice and fly ash incorporation on high temperature resistance of cement based mortars. Cem Concr Res 2007;37:988–95.

[41] El-Didamony H, Heikal M, Al-Masry S. Effect of delaying addition time of SMF superplasticizer on the physic-mechanical properties and durability of cement pastes. Constr Build Mater 2012;35:261–9.

[42] Aiad I, El-Didamony H, Heikal M, Al-Masry S. Effect of delaying addition time of synthesized SSPF condensate on the durability of sulphate resisting cement pastes incorporating micro-silica. Constr Build Mater 2013: 1092–103.

[43] El-Didamony H, Aiad I, Heikal M, Al-Masry S. Impact of delayed addition time of SNF condensate on the fire resistance and durability of SRC–SF composite cement pastes. Constr Build Mater 2014;50:281–90.

[44] Ibrahim KR, Hamid R, Taha MR. Fire resistance of high-volume fly ash mortars with nanosilica addition. Constr Build Mater 2012;36:779–86.

[45] ASTM Designation: C191. Standard method for normal consistency and setting of hydraulic cement. ASTM Annual Book of ASTM Standards; 2008.

[46] Abd-El Aziz MA, Heikal M, Abd El Aleem S. Physico-chemical and mechanical characteristics of pozzolanic cement pastes and mortars hydrated at different curing temperatures. Constr Build Mater 2012;26:310–6.

[47] El-Didamony H, Abd-El Eziz M, Abd El Aleem S, Heikal M. Hydration and durability of sulfate resisting and slag cement blends in Qaron's Lake water. Cem Concr Res 2005;35:592–1600.

[48] Abd-El-Eziz MA, Heikal M. Hydration characteristics and durability of cements containing fly ash and limestone subjected to Qaron's Lake Water. Adv Cem Res 2009;21(3):91–9.

[49] ASTM C109. Strength test method for compressive strength of hydraulic cement mortars; 2007.

[50] Land G, Stephan D. The influence of nano-silica on the hydration of ordinary Portland cement. J Mater Sci 2012;47:1011–7.

[51] Sáez del Bosque Isabel F, Martín-Pastor Manuel, Martínez-Ramírez Sagrario, Blanco-Varela María Teresa. Effect of temperature on C_3S and C_3S + nanosilica hydration and C–S–H structure. J Am Ceram Soc 2013;96(3):957–65.

[52] Hadi Bahadori, Payam Hosseini. Reduction of cement consumption by the aid of silica nano-particles (investigation on concrete properties). J Civil Eng Manage 2012;18(3):416.

[53] Heikal M, Abd El Aleem S, Morsi WM. Characteristics of blended cements containing nano-silica. HBRC J 2013;9:243–55.

[54] Abd El Aleem S, Heikal M, Morsi WM. Hydration characteristics, thermal expansion and microstructure of cement pastes and mortars containing nanoSiO_2. Const Build Mater 2014;59:151–60.

[55] Bosiljkov VB. SCC mixes with poorly graded aggregate and high volume of limestone filler. Cem Concr Res 2003;33(9):1279–86.

[56] Neville AM. The properties of concrete, ELBS. 3rd ed. Pitman Books Limited; 1983. p. 276.

[57] Heikal M. Effect of calcium formate as an accelerator on the physico-chemical and mechanical properties of pozzolanic cement pastes. Cem Concr Res 2004;34(6):1051–6.

[58] Morsy MS, Galal AF, Abo-El-Enein SA. Effect of temperature on phase composition and microstructure of artificial pozzolana cement pastes containing burnt kaolinite clay. Cem Concr Res 1998;28(8):1157–63.

[59] Walters GV, Jones TR. Effect of metakaolin on alkali-silica reaction (ASR) in concrete manufactured with reactive aggregate durability of concrete. In: 2nd Inter. Conf. Montreal, Canada, Maihotra, Ed., ACI Sp 1991;2:941.

[60] Piasta J, Sawicz Z, Rudzinski L. Changes in structure of hardened cement pastes due to high temperature. Mater Struct 1984;17(100):291–6.

[61] Chan YN, Pen GF, Anson M. Residual strength and pore structure of highstrength concrete and normal strength concrete after exposure to high temperatures. Cem Concr Comp 1999;21:23–7.

[62] Komonen J, Renttala V. Effect of high temperature on the pore structure and strength of plain and polypropylene fiber reinforced cement pastes. Fire Technol 2003;39:23–34.

[63] Alonso C, Fernandez L. Dehydration and rehydration processes of cement paste exposed to high temperature environments. J Mater Sci 2004;39(9):3015–24.